Julio J. Melero (Editor) melero@unizar.es Received and published: 17 October 2019

Dear authors, please post your response to the reviewers comments.

I kindly ask you to address the point recommendations given by both reviewers in order to let me evaluate in detail the modifications that you incorporate in the final paper.

The authors would like to thank the two anonymous reviewers for their helpful comments. Our responses are enumerated below in bold, aligned to the right side of the page. In cases where the line number of an edit has changed from the previous version of the manuscript, the new line number is included [in square brackets]. A tracked-changes version of the manuscript is included, below.

Anonymous Referee #1
General Comments
This paper computes the energy of impact to wind turbines by rain and hail, a topic that is seldom discussed, yet very important to operation and maintenance of wind farms. It points out the potential for these hydrometeors to erode the leading edge of wind turbines. They leverage public data for the US regarding dual-pol radar data and estimate the energy for typical turbine parameters. This paper should be of interest to readers of WES. The work is well-justified, interesting, and well presented. The authors justify that the problem is important and review the subject appropriately. The calculations are appropriate, but quite conservative, as the tip speed is used in computing the energy of impact. In fact, the tip itself would be seldom hit. It may be useful to provide a range of impacts as a function of distance from the hub.

Specific Comments (page and line numbers refers to tracked changes version of the manuscript)
1. The literature review is appropriate, but one wonders how much similar research has been done by the insurance industry regarding damage to cars and roofs.
   This is an excellent point. New text (and references) has been added to the introduction that documents economic losses for the USA [Page 1 Lines 27 to Page 2 Line 5]
2. This paper focuses on the U.S. It would be helpful to discuss how it is expected to apply in other parts of the world.
   The extent of RADAR coverage and the frequency of hail are both reasons why a study like this one makes particular sense in the US. We have added a sentence (and a reference) about the comparatively high frequency of hail events in the central US [Page 2 Lines 1-3] and information about broader applicability (e.g. to the European RADAR network to the conclusions [Page 17-18]
3. P. 3, line 11 – reference to the work of Bech et al. for Denmark on curtailment is interesting. Did they do a cost-benefit analysis? Readers may be interested.
   Yes, they did. Bech et al. found their curtailment strategy to be cost effective. This has been added to the introduction [page 3 line 26-30]
4. P. 5, line 5 – It would be interesting to comment on the accuracy of the current classification methods of the dual pol radars – it used to be rather poor, but may have improved with time.
   Good point. A sentence on improvements in classification has been added. [Page 5 line 25-27]
5. P. 6, line 7 – Please clarify what you mean by the "largest values". Do you mean the 75% from the prior page? Later on line 15, you refer to a fitting parameter for D_{75}, which suggests that.

Yes. Thank you. This has been made explicit. [Page 6 Line 17-19]

6. P. 6, line 29 – "the mean RPM begins to decrease at wind speeds below the cut-out velocity …" Is this true? Please provide references. The power remains constant at rated capacity until nearly at cut-out, so how does the RPM decrease? Or do you mean as it approaches cut-out speed? Please clarify

This is based on our analysis of SCADA data. There are a significant number of below-rated-RPM events for wind speeds approaching cutout. This passage has been re-worded to clarify. [Page 7 Line 21-22]

7. P. 7, line 6 – The rest of the analysis uses the speed of the blade tip for calculations. What if you used the mid-point of the blade instead as a more representative speed? You do mention that this is "conservative". It would be informative to compare the speed at the mid-point to help show the variability across the blade. Or even to plot impact as a function of distance from the hub.

Leading edge erosion is primarily of concern at or near the blade tip. An explanation (including the fact that local blade speeds vary linearly with distance from the hub) and reference have been added. [Page 7 Lines 36-38]

8. P. 15 – lines 19-p. 16, line 10 - -This is a nice list of limitations. Thanks for providing.

Thank you.

Technical corrections

9. P. 1, line 26 – please write out "approximately" (not approx..)

Done. Thank you.

10. Throughout – please add space between references in parentheses

Done

11. Throughout – it is difficult to follow and remember the 4-letter designations for the radar sites, even for an American reviewer. It will likely be even more difficult for international readers. Perhaps using the states where they are located in your references to the sites would enhance readability??

Good idea. We have added state abbreviations to the RADAR station codes throughout the text and figures.

12. P. 2, line 30 – WT was already defined

Thank you 'WT' is now used here without the redundant definition [Page 3 Line 3]

13. P. 2, line 35 – please specify U.S. Central Plains – this in an international journal.

Thank you, this has been added [Page 3 lines 9-10]

14. P. 3, line 6 – please define CONUS first time it is used.

Done [Page 1 Line 29-30].

15. P. 4, line 9 – "nominal wind farm located within the observation areas of six RADARS" is confusing. Are you referring to a wind farm for each of the six RADARS? What do you mean by "nominal" wind farm? Is this "notional"? Have you identified a specific wind farm or are you referring to one within the reach of the radar beam? As written, it implies that you have identified a wind farm that is reached by the beams of all 6 radars, which is surely not what you meant to say.

Thank you, the wording has been changed to make it clear that there 6 actual wind farms, each covered by a RADAR station [Page 4 lines 12-15]

16. P. 5, line 17 – I don't think you mean to refer to Fig. 3 here.

This reference to Fig 3 has been removed [Page 6 Line 7]

17. P. 6, line 11 – "hailstones" should be plural

This has been corrected [Page 7 line 1]

18. P. 6, line 13 – "sampled IN Alberta"

Yes, thank you. Done. [Page 7 Line 4]

19. P. 6, line 27 – "wind speed AS shown in …"

Done. [Page 7 Line 18]

20. P. 11, line 10 – hail storms are quite frequent in Boulder, Co which is just west of 105°

'Very infrequent' has been softened to 'much less frequent', which is still consistent with the literature cited (Cintineo et al and Allen and Tippett) [Page 12, Line 20]

21. P. 12, line 7 – occurring in fewer that …" (not few). The point you make here is certainly true for damage to roofs and cars.

Thank you. This has been corrected [Page 14, line 5]

22. P. 15, line 5 – " it is flexible to use with different …" (not "of")

Corrected. [Page 17, line 2]

23. P. 15, line 12 – please indent paragraphs.

Done. Thank you. [Page 17, Line 11]

24. P. 16, lines 5-7 – The word "herein" is used 3 times in 3 lines.

The wording has been changed to avoid this repetition. Thank you. [Page 17, Lines 26 to 29]

Anonymous Referee #2

The paper by Letson et al. presents an interesting study on an emerging research field related to wind energy. It is of high value for readers of WES. The methodology is presented in a clear way. The results are discussed at a high level with many papers cited within the cross-cutting field. The results are novel. The conclusion summarizes in outstanding way the many learnings and perspectives for further research. The paper is recommended for publication.

Minor edits (page and line numbers refers to tracked changes version of the manuscript)

1. P.1, line 26. Would the repair cost be different between on- and offshore wind farms? Please clarify.

Text (and a reference) has been added about the higher cost of maintenance for offshore turbines [Page 1 lines 27-28]

2. P. 2, line 38. Another challenge than age alone could be US East Coast wind farms. Please elaborate.

A sentence has been added highlighting the fact that increased blade length and O&M costs will both be more pronounced offshore. [Page 3 lines 6-7]

3. P. 3, Figure 1. As also suggested by Reviewer 1, the naming of radar stations is confusing. The naming could for simplicity be the state names (ID, TX, IL, WI, MI and NY) as you selected only one radar station in each state. For clarity, the full station names could be given once. You have selected a wind farm within a radius of roughly 60 km from each radar station. Would it be possible to add circles of this dimension at each station in the map?

We have added state abbreviations to the 4-letter RADAR station codes throughout the figures and text of the paper. We have elected to keep the 4 digit station codes as well, since these uniquely identify the RADAR stations. Since we have been provided with wind farm data under an NDA and the provider states that their wind farms must not be identified, we have not included the suggested circles around each RADAR station.

4. P. 5, line 1. Hourly precipitation rate (N1P). Did you average to 1 hour or is the data in the database 1-hour data?

Precipitation rates are only 'hourly' in that they have units of mmhr^{-1}. The wording has been changed to avoid this confusion. Thank you. [Page 5 Line 22]

5. P. 5, line 8. Is the NCR maybe Normalized Composite Reflectivity?

Nearly all of the 3-character codes for general NEXRAD RADAR products begin with an N. I believe it stands for NEXRAD. The list of codes can be found at https://www1.ncdc.noaa.gov/pub/data/radar/RadarProductsDetailedTable.pdf. This gives NCR as "Composite Reflectivity (16 Levels)"

6. P. 5, line 20. Is the spatial mean based on 5-minute and 6-minute values, then averaged to hourly?

Precipitation rates are calculated every 5-6 minutes. We have updated the text to make this clear. [Page 6 Lines 9-10]

7. P. 6, line 4, m-4. Do not use italic.

Corrected. Thank you [Page 6 line 14]

8. P. 6, line 14, would smaller be more correct than small?

Yes. Smaller is correct. This change has been made [Page 7 Line 5]

9. P.6, line 16, : : :the slope of the with hydrometeor diameter.. I wonder if "with" is a good formulation here

This has been edited ('with' removed)

10. P. 6, line 16: : :is considerably shallower than: : :. Would it be more clear to say nearly constant?

The fact that the slope is non-zero is important, and the hail number density does decrease by about 2 orders of magnitude over the radius range shown. We are more comfortable with 'shallower'.

11. Figures 3 to 7. The graphics are good but can be improved. Please use capital letter at the legends at all axis.

Axis labels and legend entries have been capitalized throughout. Thank you.

12. Fig. 4, upper panel. You show values at 0 mm/hour. Is this indicating all events with no precipitation (or from >0 but smaller than 5 mm/hour). Please clarify. Add simplified station names.

Thank you for pointing this out. The lowest tick label has been changed to < 2.5 mm/hr.

13. Fig. 5 and Fig. 7. Add simplified station names.

State abbreviations have been added for each RADAR station.

14. Fig. 6, Add simplified stations names near each of the colored markers, if possible.

State abbreviations have been added for each RADAR station here, as well

15. Page 9. The discussion of the mean wind speed for all cases at six stations from three information sources and in addition wind speed for rainy cases for six stations from one source. It is a bit confusing. A table summarizing the relevant numbers could be easier for readers to follow the discussion.

Table 2 (Page 12) has been added summarizing the mean wind speed at each site, as well as mean wind speeds conditionally sampled precipitation by the presence or absence of precipitation

16. P.6 line 7 and P. 16, line 2 you write 'conservative'. I am in doubt what you mean in this context. Please clarify.

These estimates are conservative in the engineering sense. They will tend to overestimate damage to blades.

Wording on page 6 has been added to make it clear that a conservative estimate of hail size and probability is an overestimate [Page 6 Line 10-12]

On [Page 17 line 38] (formerly page 16 Line 2), the meaning of the statement that the estimate is conservative is explained parenthetically near the end of the sentence.

RADAR-Derived Precipitation Climatology for Wind Turbine Blade Leading Edge Erosion

Frederick Letson[1] (ORCID: 0000-0001-9275-0359), **Rebecca J. Barthelmie[2] (ORCID: 0000-0003-0403-6046)**, **Sara C. Pryor[1] (ORCID: 0000-0003-4847-3440)**

[1]Department of Earth and Atmospheric Sciences, Cornell University, Ithaca, New York

[2]Sibley School of Mechanical and Aerospace Engineering, Cornell University, Ithaca, New York

Correspondence to: F. Letson (fl368@cornell.edu) and S.C. Pryor (sp2279@cornell.edu)

Abstract: Wind turbine blade leading edge erosion (LEE) is a potentially significant source of revenue loss for windfarm operators. Thus, it is important to advance understanding of the underlying causes, to generate geospatial estimates of erosion potential to provide guidance in pre-deployment planning and ultimately to advance methods to mitigate this effect and extend blade lifetimes. This study focusses on the second issue and presents a novel approach to characterizing the erosion potential across the contiguous USA based solely on publicly available data products from the National Weather Service dual-polarization RADAR. The approach is described in detail and illustrated using six locations distributed across parts of the USA that have substantial wind turbine deployments. Results from these locations demonstrate the high spatial variability in precipitation-induced erosion potential, illustrate the importance of low probability high impact events to cumulative annual total kinetic energy transfer and emphasize the importance of hail as a damage vector.

1 Introduction and objectives

In 2017 wind turbines (WT) provided 6% of total electricity generation in the United States of America (USA) (U.S. Energy Information Administration, 2018) and there are over 50,000 WT operating in the USA today (Pryor et al., 2019). WT are subject to harsh operating conditions during their 20-25 year lifetimes including; extreme winds, impacts from heavy rain, hailstones and snow, and intense ultraviolet light exposure that can lead to material damage (Keegan et al., 2013). Accordingly, operation and maintenance (O&M) costs comprise 20-25% of the total levelized cost per kWh of electricity produced over the WT lifetime (Mishnaevsky Jr, 2019; Moné et al., 2017). WT blades exhibit the highest failure rate (FR ~ 0.2) of any WT component (Zhu and Li, 2018). The most expensive repair and longest repair times are associated with blades (Shohag et al., 2017). Estimates suggest average cost of blade repair of an onshore turbine is approximately $30,000, with replacement costs of ~ $200,000 (Mishnaevsky Jr, 2019). Repair and replacement costs will tend to be higher offshore where general O&M costs are higher (~30% of total cost) and blade failures contribute also significantly to turbine downtime (Carroll et al., 2016).

Hail has long been recognized as an important source of weather-related economic losses in the Contiguous United States (CONUS) (Changnon, 1999; Cintineo et al., 2012). Economic losses from hail were estimated to be $1.2 billion in 1999 (Changnon, 1999), and property damage from severe hail has been shown to be increasing with time (Changnon, 2009), with more recent annual losses estimated at $10 billion, accounting for almost 70% of severe-weather-related insurance claims (Loomis, 2018). An analysis conducted in 2009 indicated an average of 159 days each year are associated with crop-damaging hail leading to average crop loss of $580 million, and hail damage to property was valued at $850 million (Changnon et al., 2009). Hail, and hail damage, are highly episodic. For example, insurance losses in the Dallas–Fort Worth (DFW) metroplex on

1

a single hail day in May 2011 were estimated to exceed $876 million (Brown et al. 2015). While the paucity and subjectivity of observed hail data sets make a global comparison difficult, severe hail is almost certainly more common in the central US than in other areas of the world with substantial wind energy development (Prein and Holland, 2018). Further, the relationship linking damage to the frequency and severity of hail varies substantially with the target. WT present an interesting challenge in this context because they are large structures and the blades are rotating, composite materials.

A key cause of the need for WT blade repairs is excess damage (i.e. material loss) on the leading edge (leading edge erosion, LEE). LEE roughens WT blades, reducing lift and electrical power production (Sareen et al., 2014; Gaudern, 2014). LEE causes an average of 1-5% reduction in annual energy production (AEP) (Froese, 2018) and up to a 9% reduction when delamination occurs (Schramm et al., 2017). Thus, excess LEE may be costing the industry tens of millions of dollars per year via lost revenue and/or increased maintenance costs, and poses a threat to achieving continuing wind energy cost reductions (Sareen et al., 2014). In response to this issue a major industrial research consortium from Europe (including DNV GL, Vestas and Siemens Gamesa Renewable Energy) has recently (Nov 2018) announced a new partnership (COBRA) focused on analysis of mitigation measures for LEE including development of next-generation leading-edge protection systems (Durakovic, 2019).

WT blades use composites (e.g. epoxy or polyester, with reinforcing glass or carbon fibers) (Mishnaevsky et al., 2017) coated to protect the blade structure by distributing and absorbing the energy from impacts (Brøndsted et al., 2005). Thus, the leading edge actually comprises several layers of the main structural composite material (and thickening materials) plus coatings (Mishnaevsky et al., 2017). Impact fatigue caused by collision with rain droplets and hail stones is a primary cause of WT blade LEE (Bech et al., 2018; Bartolomé and Teuwen, 2019; Zhang et al., 2015). Although rain droplets fall at only modest velocities (typically $\leq$ 10 ms^{-1}, see details below), the tip of WT blades rotate quickly (50-110 ms^{-1}), thus the net closing velocity and kinetic energy transfer are large. Each precipitation impact on the blade leading edge results in transient stresses that are proportional to impact velocity (Preece, 1979; Slot et al., 2015). The stress induced by individual high net collision impacts with hydrometeors may, in principle, exceed the strength of the material. Estimates of the failure energy threshold of a composite structure vary widely (e.g. values of 72 – 140 J are given in (Appleby-Thomas et al., 2011)) and may exceed 300 J for leading-edge thicknesses and hailstone diameters > 20 mm (Kim and Kedward, 2000). However, conceptually the erosion of homogeneous materials is most frequently considered using a three stage model. Initially there is an incubation period during which impacts occur but no visible damage is observed although microstructural changes in the materials generate nucleation sites for material removal which commences when a threshold is reached (i.e. when some level of accumulated impacts is reached). Once the time to damage has been exceeded additional damage occurs as stress waves propagate from the impact sites into the composite and cause existing pits and cracks to grow and there is a steady increase of material loss occurs with each additional impact (Cortés et al., 2017; Eisenberg et al., 2018; Traphan et al., 2018). The number of impacts required to reach the threshold for surface fatigue failure is a function of the droplet diameter and phase, the closing velocity, the strength of the material and the pressure of the impact. Hence, the materials response to hail (solid hydrometeors) may differ from that to collisions with liquid (rain) droplets. For example, the maximum von-Mises stress created in the WT blade leading edge from a 10 mm diameter hailstone greatly exceed that from a rain droplet of equivalent size and closing velocity due to differences in mass and hardness (Keegan et al., 2013).

WT LEE is a developing area of research and uncertainty remains regarding frequency and severity of the issue. Rates of LEE appear to be highly spatially variable due to variations in WT operating conditions and the precipitation climate. Industrial experience has demonstrated exposure to particularly harsh operating conditions can erode coatings causing partial delamination after as little as 2-3 years (Rempel, 2012; Keegan et al., 2013). Elastomeric coatings can be applied for additional erosion resistance (Dalili et al., 2009; Valaker et al., 2015; Herring et al., 2019). However, the life of such coatings cannot be predicted

2

Deleted: Estimates of total annual hail damage to property and to crops in the Contiguous United States (CONUS) exceed $1 billion, and threlationship

Deleted: of

Deleted: with the type of target

Deleted: (Changnon, 1999;Cintineo et al., 2012)

Deleted: Being

Deleted: structures

Deleted: , WT present a unique challenge in understanding the connection between precipitation conditions and degree of damage

accurately (and is a function of UV exposure, (Shokrieh and Bayat, 2007)), they have a negative impact on blade aerodynamics (Giguère and Selig, 1999) and their cost-effectiveness is uncertain (Dashtkar et al., 2019).

The total installed capacity (IC), rated capacity (and physical dimensions) of WT being installed exhibited marked growth in the USA over the last 20 years (Wiser and Bolinger, 2018; Wiser et al., 2016). Average WT blade length increased from < 4 m in 1985 to 32 m in 2005 and now exceeds 55 m (Wiser and Bolinger, 2018). Since the tip speed increases with blade length, this tendency towards taller WT with longer blades exacerbates LEE potential. The increased blade length and larger maintenance costs associated with offshore wind turbines tend to make offshore wind farms especially vulnerable to LEE. Based on previous research the *a priori* expectation of this research is that excess LEE is most likely on WT deployed in environments with high rain intensities and hail frequencies such are experienced in the Great Plains (the states of Texas (TX), Oklahoma (OK), Kansas (KS), Nebraska (NE), North and South Dakota (ND, SD), Wyoming (WY) and Montana (MN); Fig. 1). LEE is likely to present a growing issue within the US wind industry as more and larger wind turbines with higher tip-speed ratios are deployed (Amirzadeh et al., 2017a). The current average age of WT in the US is 9 years (AWEA, 2019) and LEE will be of greater concern as a larger number of WT move out of the typical 1 to 5 year warranty period (Bolinger and Wiser, 2012; Brown, 2010).

Addressing the challenges posed by blade LEE and developing mitigation options requires multi-scale and multi-disciplinary research. Given the importance of precipitation phase, size and intensity during WT operation to the potential for blade LEE here we focus on developing a consistent and generalizable framework that can be applied to derive estimate of erosion-relevant atmospheric properties. We present an objective, spatially consistent, robust and repeatable framework that can be applied across CONUS and crucially uses only non-commercial (i.e. publicly available) data. The specific objectives of the research reported herein are:

1) To develop the workflow necessary to develop a proto-type RADAR-based erosion atlas.
2) To provide a first estimate of the spatial variability of erosion potential across CONUS in regions where wind turbines are currently deployed (see Fig. 1).
3) To conduct an initial uncertainty propagation exercise to illustrate how uncertainties in the input data propagate through the analysis workflow to influence erosion potential estimates.
4) To describe the degree to which blade LEE is episodic and therefore amendable to the mitigation strategy proposed earlier in research from Denmark of WT curtailment during 'highly erosive' periods. The efficacy of this strategy is a function of (i) the wind speed regime and joint probability distributions of erosive events (heavy rain or hail) and power-producing wind speeds, (ii) price of electricity supplied to the grid and (iii) O&M costs. A cost-benefit analysis based on conditions in Denmark suggested the loss of revenue from the curtailment of power production was small compared to the economic benefits from enhance blade lifetimes (Bech et al., 2018).

3
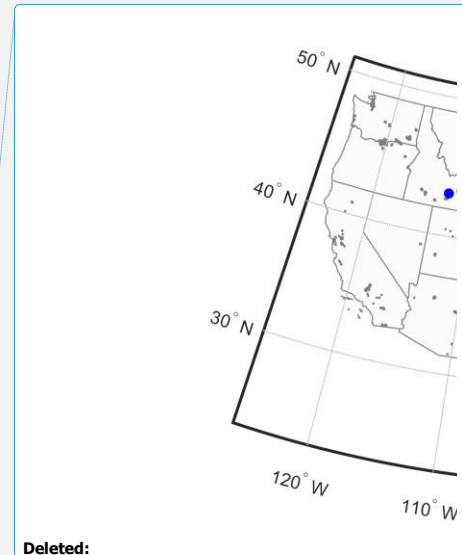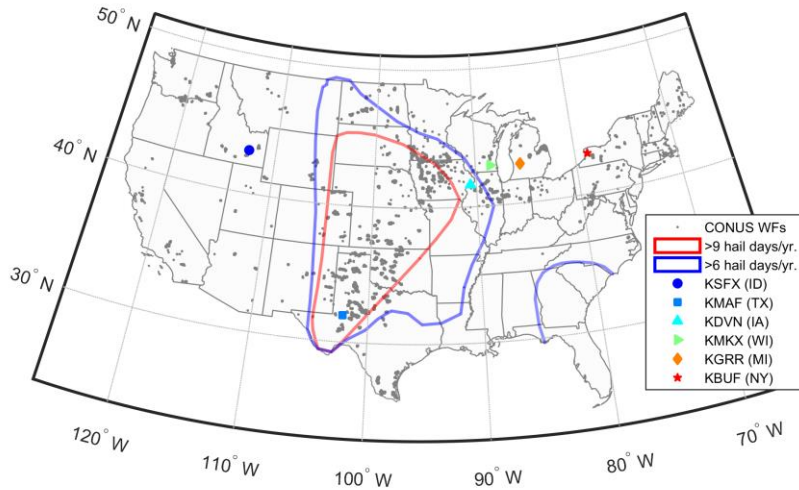
Figure 1 Locations of wind turbines as deployed at the end of 2017 according the UGSGS database (available from; https://eerscmap.usgs.gov/uswtdb/) (grey dots), the NWS RADAR stations from which data are presented (see details in Table 1), and areas of frequent hail occurrence. Areas with more than nine hail days per year are outlined by the red contour, and those with more than six are outlined by the blue contours (Cintineo et al., 2012).

Table 1: The station code and locations of the six NWS dual polarization RADARs from which data are presented (listed from west to east).

Station code	Latitude (N)	Longitude (E)	State
KSFX	43.106	-112.686	ID
KMAF	31.943	-102.189	TX
KDVN	41.612	-90.581	IA
KMKX	42.968	-88.551	WI
KGRR	42.894	-85.545	MI
KBUF	42.949	-78.737	NY

2 Data and Methods

A first estimate of precipitation-derived erosion potential at sites across the USA as developed in the current work is based on a characterization of the kinetic energy exchange from rain and hail impacts on the blade leading edge. The procedure used in making these estimates is divided into two steps: Calculation of meteorological parameters (wind speed, rain and hail) at six wind farms, each located within the observation area of a RADAR station, and then calculation of blade impact frequencies and energy transfer based on those meteorological parameters. Exact wind farm locations and details are excluded from this paper under a non-disclosure agreement (NDA).

4

The research reported herein leverages resources generated from the upgraded National Weather Service (NWS) network of WSR-88D RADAR to dual polarization (completed in 2013, (Seo et al., 2015; Crum et al., 1998)) along with the NOAA Weather and Climate Toolkit (WCT) (see details of the data products and data volumes provided in Appendix A). These data represent a unique opportunity to characterize precipitation properties such as hail that are very challenging to detect and to

5 accurately characterize using in situ methods or human observers (see discussion in (Allen and Tippett, 2015) and details of RADAR operation (Kumjian, 2018)). NWS RADAR operate at elevation angles between 0.5° and 19.5° and an azimuthal resolution of 1°. Doppler and dual-polarization data are publicly available at a resolution of 0.25 km up to a range of 300 km from each RADAR site (NOAA, 1991; Istok et al., 2009) (see description of the data provision in (Kelleher et al., 2007) and an example of the NWS products given in Fig. 2). The temporal resolution of the data is typically ~ 5 minutes, but varies slightly

10 with scanning mode: 1) Clear Air Mode uses longer, 10-minute scans to collect sufficient return data during times of no precipitation when signal return strength is relatively low. 2) Precipitation mode is used when there is any precipitation detected in the scan area and uses a 6-minute scan cycle. 3) Storm mode is used when severe or rapidly-evolving storms are present, and uses a 5-minute sampling interval, made possible by reducing the number of elevation angles used (NOAA, 2016a). Storm detection and tracking using RADAR is a complex and evolving science but in brief the NWS system uses an automated function

15 which employs reflectivity from the current scan and storm cell location and vertically integrated liquid water (VIL) from the previous scan (Johnson et al., 1998).

To illustrate the proposed analysis framework we use data from six NWS dual-polarization Doppler RADAR stations (see Fig. 1 and Table 1) collected over the period 2014-2018. These locations were chosen to represent gradients in hail probability and precipitation amount in regions with relatively high wind turbine installed densities (Fig. 1). We employ the framework in

20 order to generate erosion climates for six wind farms operating in the scanned volume of the RADARs and located 35-75 km from the RADAR locations. The following RADAR data products are used (see also Appendix A):

- Precipitation rate (N1P) is the precipitation rate in each RADAR cell in each ~ 5 minute period (expressed in units of mmhr^{-1}) as estimated from reflectivity.

- Hybrid Hydrometer Classification (HHC): Based on reflectivity, temperature, and dual polarization variables, HHC is an

25 estimate of the most likely targets within the RADAR volume. While this is derived product, classification algorithms and accuracy have improved with the widespread adoption of dual polarization RADAR and application of areal (rather than point-wise) techniques (NOAA, 2016b; Chandrasekar et al., 2013). The hydrometeor types encoded in the NWS data product are; dry snow, wet snow, crystals, big drop, rain (light and moderate), heavy rain, graupel, and rain with hail.

- Hail reports (NHI): Maximum hail size (an estimate of the 75th percentile hail stone diameter (D_{75})) and probability of hail

30 are used to identify the occurrence and severity of hail events (see discussion in (Witt et al., 1998)).

- Composite Reflectivity (NCR): Maximum reflectivity at any elevation angle measured in each RADAR cell. This is used here to characterize the spatial extent of hail events (i.e. reflectivity > 50 dBZ (Witt et al., 1998)).

- Radial wind speeds from the 0.5° elevation angle as computed from the Doppler shift (N0V) (Alpert and Kumar, 2007).

Deleted: nominal

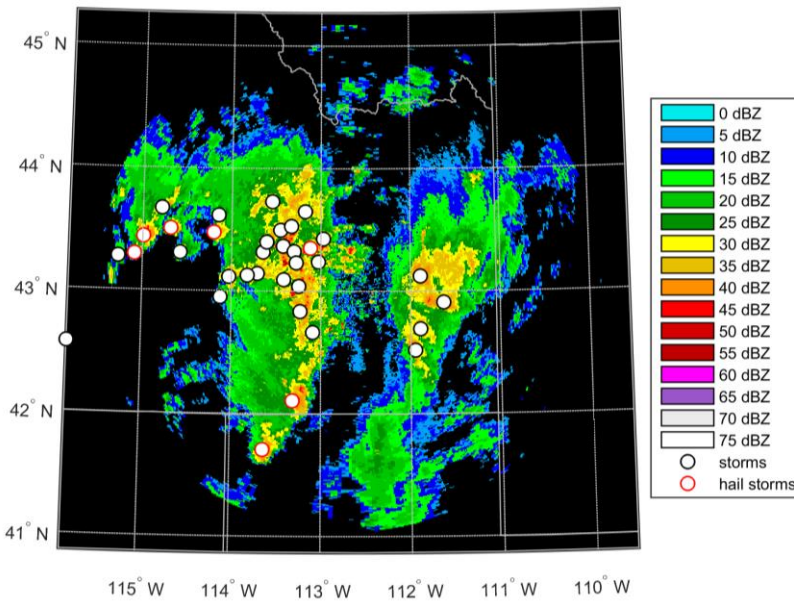**Deleted:** Hourly p

Deleted:

Deleted: C

5

Figure 2 – Example of a single five minute period of RADAR data from KSFX (ID; August 8, 2013, 22:37 UTC). The colors show the composite reflectivity (i.e. the maximum reflectivity from any of the elevation angles sampled by the NWS RADAR) in dBZ. The circles represent storm cells that are identified and tracked by the NWS detection algorithm; black circles are storms without hail, and red circles are those with hail.

Wind speeds, hydrometeor type and precipitation intensity for each nominal wind farm located within each RADAR scanned area in each five minute period are derived as follows:

Precipitation intensity is characterized by rainfall rate (*RR*) in mmhr⁻¹, which is derived using RADAR Z-R relationships (Wilson and Brandes, 1979) and reported in the parameter precipitation rates (N1P) in all RADAR cells every ~ 5 minutes. A spatial mean of all N1P values in all RADAR cells within 5 km of the wind farm centroid is used here. This rainfall rate is also used to derive the raindrop spectrum using the Marshall-Palmer distribution (Marshall and Palmer, 1948). In it the number of droplets above radius, *R*, per cubic meter of air (*N*, m⁻³) is given by;

$$N = \frac{N_0}{\Lambda} e^{-\Lambda R} \tag{1}$$

Where $\Lambda = 8200(RR)^{-0.21}$ (m⁻¹), *RR* is the rainfall rate in mmhr⁻¹, and $N_0 = 1.6 \times 10^7 \text{m}^{-4}$. See an example rain droplet size distribution, expressed as *dN/dR*, for a *RR* of 25 mmhr⁻¹ in Fig. 3.

Hail occurrence is characterized by a number of NWS RADAR-derived parameters, most of which are contained in the hail reports (NHI). Hail size and probability of occurrence are conservatively estimated here, by taking the largest D_{75} value and hail probability reported for any storm cell within 5 km of the nominal wind farm centroid (which will tend to bias both toward higher values). The spatial coverage of hail within that 5 km radius is determined by calculating the fraction of RADAR cells in that area which have composite reflectivity in excess of 50 dBZ. Hail size distributions are relatively uncertain but are generally

6

considered to be exponential up to a ceiling diameter (Auer, 1972; Lane et al., 2008). Herein the size distribution of hailstones is assumed to follow (Cheng and English, 1983):

$$N(D) = 115\lambda^{3.63}e^{-\lambda D} \qquad (2)$$

where D is the hailstone diameter (Cheng and English, 1983). This formulation is based on seven events sampled in Alberta, Canada which covered a smaller diameter range than indicated by the RADAR products, but it has the advantage that the distribution requires a single fitting parameter (λ) and thus can be fully described using only D_{75}. As shown by the example hail distribution (expressed in dN/dR) for $D_{75} = 25$ mm and $\lambda = 0.053$ mm^{-1} (Fig. 3), the slope of the hydrometeor diameter is considerably shallower than for rain droplets as described using Marshall-Palmer. In order to avoid the occurrence of extremely large hailstones, we truncate the distribution to include diameters up to two times the RADAR-estimated 75th percentile hail stone diameter (D_{75}). The presence of such a hail-size ceiling is consistent with previous observations (Auer, 1972).

Wind speeds from RADAR have been previously used for numerical wind resource verification (Salonen et al., 2011). Wind speeds at a typical wind turbine hub-height of approximately 80 m are derived using the radial wind speeds from the 0.5° elevation angle scan at a distance of 8 km ($\pm$ 0.5 km) range from the RADAR station using an assumption of uniform flow from:

$$V_{radial}(\theta) = V_{mean}\cos(\theta) \qquad (3)$$

where θ is the difference in angle between the RADAR beam and the direction of mean flow, and V_{mean} is the mean wind speed at hub height. A least-squares fit of a sinusoid of this form is made to each wind speed scan (excluding cells which report a zero wind speed) to estimate V_{mean}. The resulting wind speed is then used within the simple description of the blade rotational speed as a function of hub-height wind speed as shown in Fig 4c. This operational RPM curve is based on long-term data provided from large operating WT arrays (under an NDA) and represents the mean rotational speed across all WT operating in these arrays as a function of the mean wind speed at hub-height across the arrays. The mean RPM decreases at wind speeds below the cut-out velocity (of 25 ms^{-1}) due to some WT rotating below their design RPM at very high wind speeds (near cut-out) as reported in the SCADA data.

Once the hydrometeor type (rain or hail), hydrometeor size (which determines mass and terminal velocity) and wind speed for a reporting period are known, hydrometeor impact energies for that period are calculated using the mass and closing velocity for hydrometeors of each radius occurring in the period. For this analysis the terminal velocity for each size of rain droplets is derived using (Stull, 2015):

$$V_{t,rain} = k\left[\frac{\rho_o}{\rho_{air}}R\right]^{1/2} \qquad (4)$$

where R is the droplet radius (m), $k = 220$ m$^{1/2}$s^{-1}, ρ_o is air density at sea level (set to a constant of 1.25 kgm^{-3}, herein), ρ_{air} is air density at the altitude above sea level at which the rain droplet is crossing the rotor plane (see example of $V_{t,rain}$ in Fig. 3). The terminal velocity of hail stones is derived using (Stull, 2015):

$$V_{t,hail} = \left[\frac{8}{3}\frac{|g|}{C_D}\frac{\rho_i}{\rho_{air}}R\right]^{1/2} \qquad (5)$$

where R is radius of the hailstone (m), ρ_i is the density of ice (set to a constant of 900 kgm^{-3} herein), ρ_{air} is air density at the altitude at which the hail is falling. $C_D = 0.55$ is the drag coefficient (Stull, 2015) (see example of $V_{t,hail}$ in Fig. 3).

Closing velocity, V_c, as a function of hydrometeor type and diameter (D) is calculated from wind speed, V_{mean}, rotor speed, V_r (calculated from wind speed and RPM curve), terminal velocity, V_t and blade position, $\phi(t)$. V_r as derived here represents the linear speed of the blade tip due to rotation, as this will lead to conservative estimates of impact energy. Local blade speeds increase linearly with distance from the hub, so both the frequency and the energy of impacts is at a maximum near the blade tip, where blades are particularly susceptible to erosion (Keegan et al., 2013).

$$V_c(D,t) = \left[V_{mean}^2 + (V_r + V_t(D) \cdot \cos(\phi(t)))^2\right]^{1/2} \tag{6}$$

The impact rate (I) on the blade leading edge as a function of hydrometeor type and size is calculated from the number density of the hydrometeors of a given diameter ($N(D)$) and the closing velocity:

$$I(D,t) = N(D) \cdot V_c(D,t) \tag{7}$$

The assumption that all falling rain droplets will impact the blade is made on the basis of evidence that only droplets with diameters below 0.2 mm have insufficient inertia to be deflected from the blade by streamline deformation (Eisenberg et al., 2018). The maximum kinetic energy transferred to the blade from the hydrometeors is then computed for each hydrometeor type and diameter using the following approximation:

$$E_K(D,t) = \tfrac{1}{2}m(D) \cdot V_c(D,t)^2 \tag{8}$$

where $m(D)$ is the mass of the hydrometeors of a given diameter.

The total kinetic energy of impacts over a time interval, T, associated with hydrometeors of diameter, D, is given by:

$$E_{K,T}(D) = \int_{t_0}^{t_0+T} I(D,t) \cdot E_K(D,t)dt \tag{9}$$

where dt is the time interval at which the RADAR measurements are available (5 minutes).

The RADAR-estimated probability of hail and the geographic extent of hailfall are both treated probabilistically with respect to the number of expected hail impacts on any particular wind turbine within the wind farm. The number of expected impacts at each kinetic energy are multiplied by two factors representing these two effects. (1) The probability of hail being associated with the storm in question, as estimated by the RADAR hail detection algorithm, and (2) the fraction of RADAR cells within 5 km of the wind farm centroid which have a composite reflectivity of > 50 dBZ, the range commonly associated with hail.
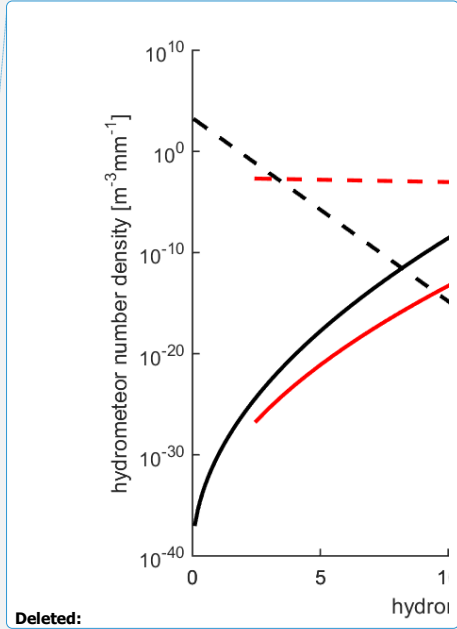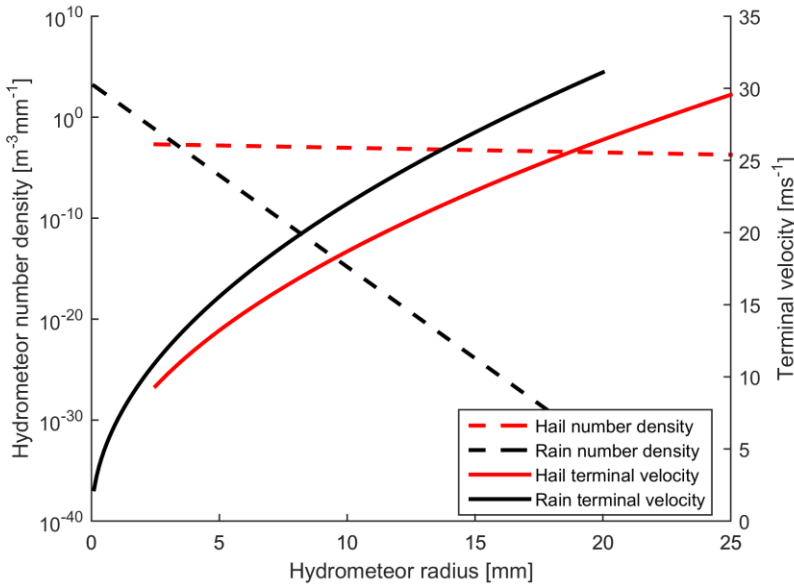
Figure 3 – Example of the hydrometeor number density (dN/dR; number of droplets per meter cubed of air per mm of radius increment) for a precipitation rate of 25 mm hr^{-1} for rain droplets (as described using the Marshall-Palmer size distribution) and for hail stones (for D_{75} of 25 mm and $\lambda = 0.053$ mm^{-1}) (left axis). Note: The λ value employed ($\lambda = 0.053$ mm^{-1}) differs from the range (λ: 0.1 to 2 mm^{-1}) used by (Cheng and English, 1983) for the seven events they sampled and thus corresponds to a larger maximum hail size. Hydrometeor terminal velocities of hail and rain are shown by radius on the right axis.

NWS RADAR products have been subject to extensive product development efforts and a wide range of evaluation exercises (Cunha et al., 2015; Villarini and Krajewski, 2010; Straka et al., 2000), but are nevertheless associated with measurement uncertainties, as are the approximations applied herein to derive terminal fall velocities and kinetic energy transfer. To provide a first assessment of how these uncertainties in input data propagate through the analysis framework and thus impact derived kinetic energy exchange each of three key parameters of the erosion potential are perturbed from 50% to 150% of observed values during two example periods of comparatively high erosion potential. The first case represents a period of large hail. In this analysis D_{75} is set to the 99th percentile D_{75} at KMKX (WI) (42 mm) and V_{mean} is set to 11.3 ms^{-1} (i.e. the mean wind speed conditionally sampled by ±10% of D_{75} = 42 mm). In the second, a heavy rain event is considered. The RR is set to the 99th percentile value at KMKX (18 mmhr^{-1}) and the V_{mean} is set to the mean value (12.8 ms^{-1}) during heavy rainfall (i.e. RR within 10% of the 99th percentile value at KMKX).

Uncertainties in RADAR-derived hail sizes are less well characterized than for V_{mean} and RR. For RR the range of ± 50% is inclusive of previously published uncertainties, understanding that those uncertainties are a function of spatial resolution, RR and RADAR processing algorithm (Seo and Krajewski, 2010; Seo et al., 2015). Wind speed uncertainty (as quantified using RMSE) for an elevation angle of 0.5° is approximately ± 3.4 ms^{-1} (Fast et al., 2008) and thus for a wind speed of 12.8 ms^{-1} a +/-50% variation is fully inclusive of the estimated wind speed error.

3   Results

Key aspects of the erosion-relevant RADAR-derived atmospheric properties at the six locations are summarized in Fig. 4. Consistent with previous precipitation climatologies, there are marked spatial gradients in the annual total and precipitation intensity (RR, Fig. 4a) (Prat and Nelson, 2015). Precipitation rates of < 5 mmhr^{-1} are common at all sites, RR of 20 mmhr^{-1} are experienced at all locations, but only the site in Texas (KMAF) exhibits any occurrence of rainfall intensity in excess of 35 mmhr^{-1}. Using a damage rate of 3×10^{-5} s^{-1} for a RR of 20 mmhr^{-1} and a closing velocity of 120 ms^{-1} (Eisenberg et al., 2018), the frequency of RR of 20 mmhr^{-1} at the site in Texas is such that it would accumulate ~ 0.6 of impact necessary to reach the transition threshold from the incubation region to material loss over a 25 year period.

At most sites, snow and ice occur at rates at least one order of magnitude less frequently than rain. The exception is the site in Idaho (KSFX) (Fig. 4d). At each of the six locations, there are fewer than 40 five-minute hail periods per year. Consistent with expectations and previous research (Cintineo et al., 2012), while hail events occur at all six sites, hail frequency and severe hail events (with maximum hail sizes > 25 mm) are substantially more frequent at the nominal wind farm locations in Texas, Illinois and Wisconsin (RADAR ID; KMAF, KDVN and KMKX) (Fig. 4b). The derived frequency distributions of wind speed close to wind turbine hub-heights (WT HH) exhibit a high frequency of wind speeds above typical wind turbine cut-in speeds, and are particularly right-skewed at the site in Iowa (Fig. 4c). The mean annual wind speed near nominal WT HH is lowest at KSFX (ID) where it is ≈ 5.9 ms^{-1}. They range from 8.6 to 10 ms^{-1} at KGRR (MI), KMKX (WI), KBUF (NY) and KDVN (IA) (Table 2). The wind speed distributions at these five of the six locations exhibit relatively good qualitative agreement with *a priori* expectations (see wind resource maps available at; https://windexchange.energy.gov/maps-data/324) and estimates from simulations for 2002-

Deleted: Illinois

Deleted: in Idaho

Deleted: listed in ascending order of V_{mean}; see also

2016 with the Weather Research and Forecasting model (Pryor et al., 2018) for 12 km grid cells containing the nominal wind field locations that indicate mean annual wind speeds of 6.5 ms^{-1} at KSFX (ID), and 8.4-9.0 ms^{-1} (KGRR (MI), KMKX (WI), KBUF (NY) and KDVN(IA)). However, wind speeds derived from RADAR observations from KMAF (TX) are relatively low (mean value of 5.9 ms^{-1}) and exhibit a relatively low frequency of observations above 13 ms^{-1} (2.2%). This negative bias (of > 1 ms^{-1} in the mean relative to the resource map and WRF model output) from the Texas site will tend to lead to lower RPM values and hence blade tip speeds and thus a negative bias in kinetic energy transfer at this location. Wind speed distributions during precipitation and no-precipitation periods are qualitatively similar at all six locations. Modal values are within +/- 1.2 ms^{-1}, but the distributions are heavier tailed at all sites during precipitation periods. Mean wind speeds during precipitation are 0.2-3.8 ms^{-1} higher at the six locations than during times of no precipitation (Table 2).
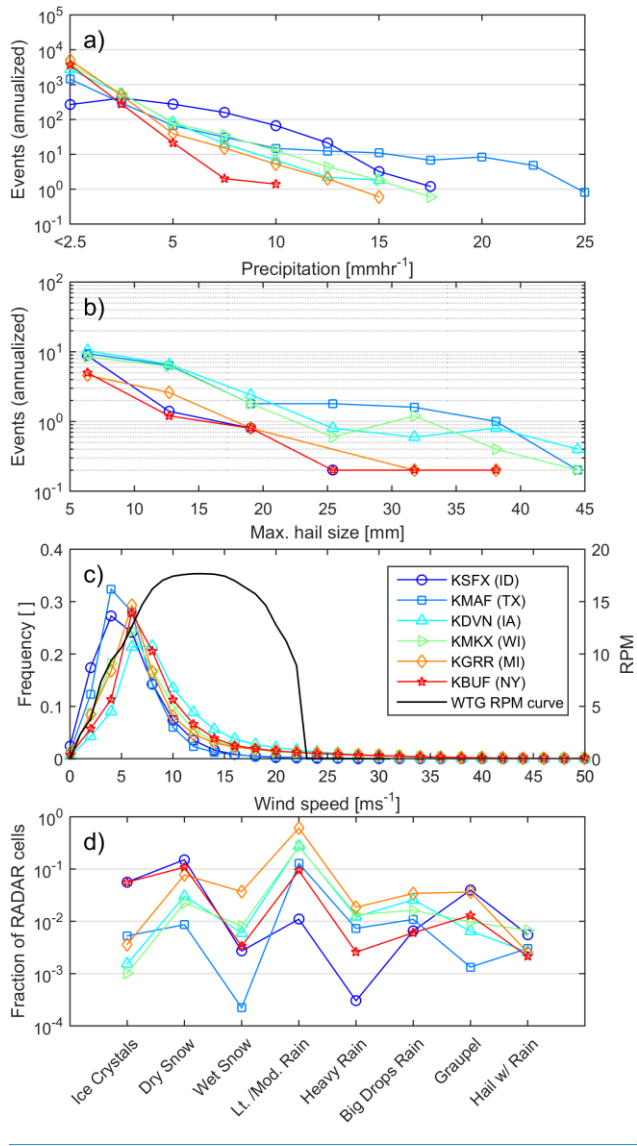
Deleted: KMKK

Deleted: ¶

Figure 4 – Precipitation and wind speed climates from RADAR data (see locations in Fig. 1). (a) Mean annual number of 5 minute periods of each _RR_ intensity class (discretized in 5 mmhr^{-1} intervals). (b) Mean annual number of 5 minute periods with maximum hail sizes (D_{75}) (discretized in 5 mm intervals). (c) Wind speed distributions for all 5-minute periods (discretized in 2ms^{-1} intervals). The black line in this frame shows the WT RPM curve as a function of wind speed (WTG RPM, right axis) (d). Occurrence of NWS RADAR hydrometeor classifications for each nominal wind farm shown as the fraction of RADAR cells in each class during all periods with _RR_ > 1 mmhr^{-1}.
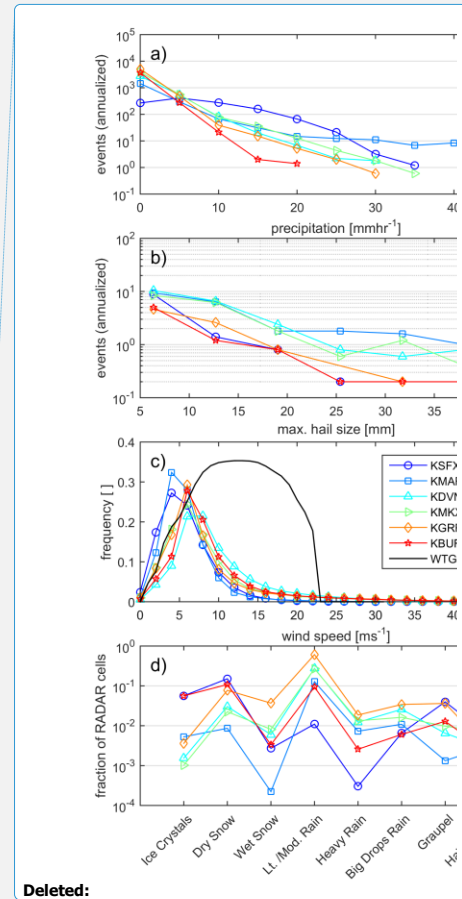
11

Table 2: Mean wind speeds close to WT HH from each RADAR: The long-term mean, V_{mean}, the mean during times of precipitation, V_p, and the mean during times of no precipitation V_{np}

Station Code	Mean wind speeds [ms^{-1}]		
	V_{mean}	V_p	V_{np}
KSFX (ID)	5.8	5.9	5.7
KMAF (TX)	5.9	6.7	5.8
KDVN (IA)	10.0	11.1	9.8
KMKX (WI)	8.8	10.2	8.7
KGRR (MI)	8.6	12.3	8.5
KBUF (NY)	9.2	10.9	9.0

Given the exponential dependence of hailstone and rain droplet size on precipitation intensity and the accumulated
5   damage therefrom (Eisenberg et al., 2018), the distributions of kinetic energy transfer from the two hydrometeor types at all sites are heavy-tailed. Further, the probability distributions of each 5-minute estimate of kinetic energy transfer (Fig. 5) and total annual kinetic energy transfer (Fig. 6) indicate marked differences between the sites and between the two hydrometeor types. Extremely high hail kinetic energies are most frequently projected for sites in Texas (KMAF), Iowa (KDVN) and Wisconsin (KMKX) (Fig 5a). This is consistent with the precipitation climatology summarized in Fig. 4b and the high frequency of wind
10 speeds associated with high WT RPM (Fig. 4c). At these three sites some events (5 minute periods) exhibit kinetic energy of transfer from hail in excess of 300 J (Fig. 5a). Although these events have a low probability (less than 1 per square meter per year), they may thus be sufficient to cause damage to blade coatings in isolation from the effects of the cumulative fatigue (Appleby-Thomas et al., 2011; Kim and Kedward, 2000). Conversely, individual rain impacts rarely exceed 5.2 J at any site. The probability of exceeding this impact kinetic energy threshold over a square meter of blade leading edge is less that 10^{-3} per year
15 (Fig. 5b). Thus, hail dominates the annualized cumulative kinetic energy of transfer to each square meter of the blades at all sites (Fig. 6). Indeed, at all sites, despite the low probability of hail relative to rain (cf. Fig. 4a and 4b), total annual kinetic energy transfer from hail exceeds that from rain by at least two orders of magnitude (Fig. 6). The lowest cumulative kinetic energy transfer is projected for the nominal wind farm sites in Idaho (KSFX), New York state (KBUF) and in Michigan (KGRR). Conversely, values are highest for in Texas (KMAF), Iowa (KDVN) and Wisconsin (KMKX). This is consistent with previous
20 characterizations of hail frequency, which show hailfall to be most common in the Great Plains, and much less frequent west of 105° west (Fig. 1) (Cintineo et al., 2012; Allen and Tippett, 2015).
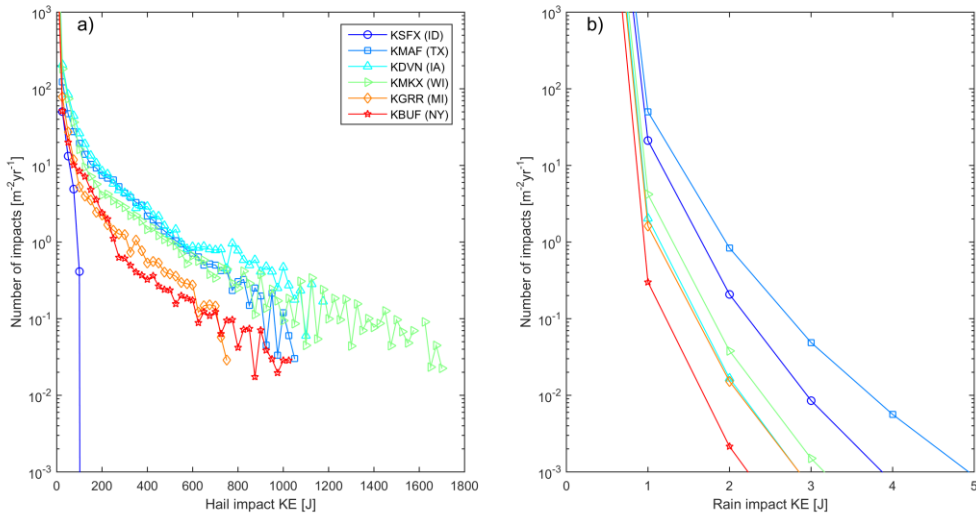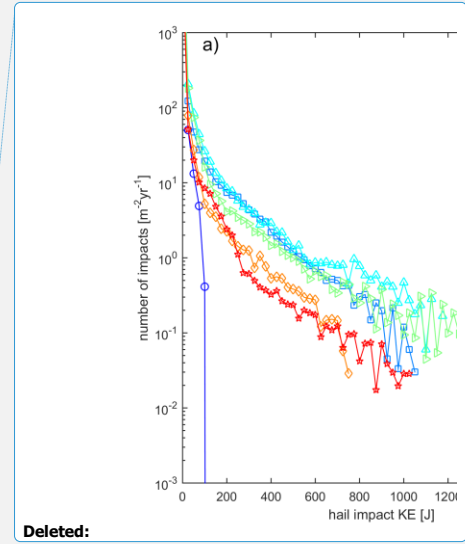
Figure 5 – Histograms of kinetic energy of hydrometeor impacts. Annual number of (a) hail and (b) rain impacts per m² of blade leading edge as a function of impact kinetic energy. The y-axis in panel (b) has been truncated to a maximum value of 1000 per year.

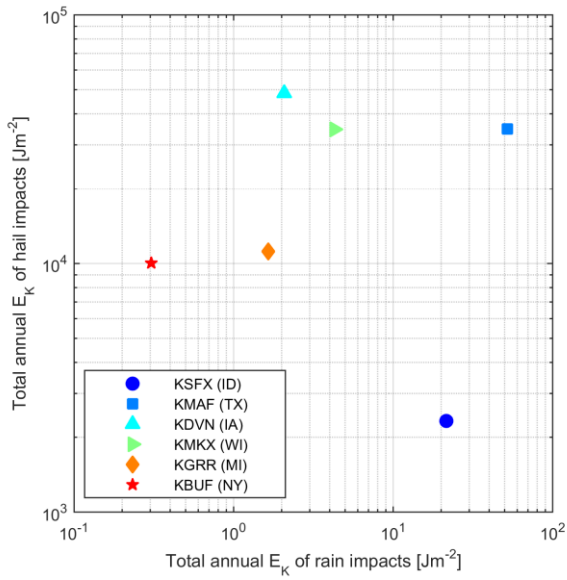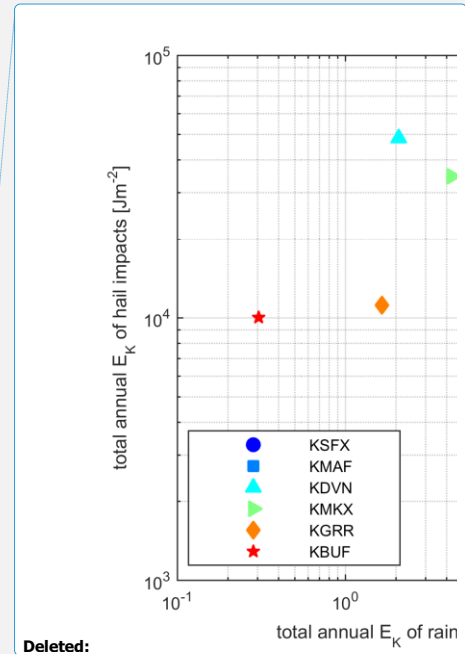**Figure 6 – Total annual kinetic energy (E$_K$) per m² of blade leading edge from rain and hail impacts at each location.**

5

13

Fig. 7 illustrates that only a very small fraction of 5-minute periods dominate kinetic energy transfer to the blades from both hail and rain. At all sites over 80% of rain-induced kinetic energy transfer occurs in the top 80 5-minute periods per year. Indeed, at all but the site in Idaho (KFSX) over half of the total rain-induced kinetic energy transfer to the blade occurs in only 20 5-minute periods in a year. The probability distribution of hail-induced kinetic energy transfer is even more heavy-tailed with at all sites 90% of the cumulative kinetic energy transfer to the blades from hail occurring in fewer than 25 5-minute periods per year. Thus, few events dominate the annual total accumulated impact damage.
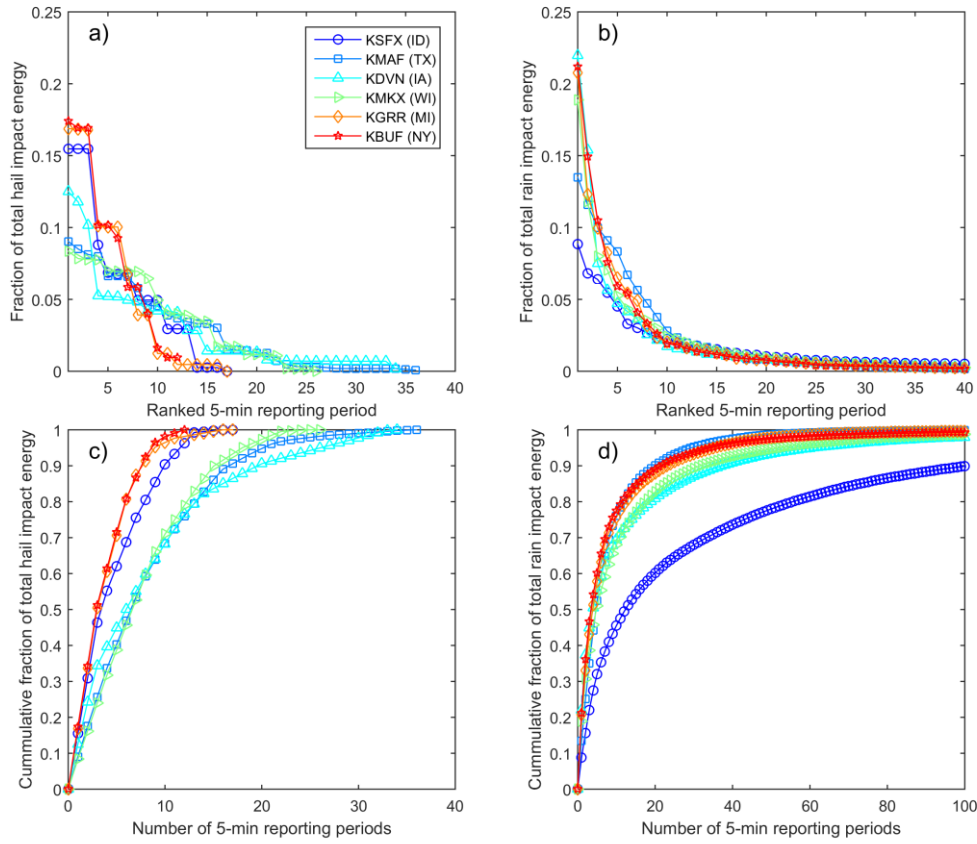
Figure 7 – Contributions of the most intense precipitation events to annual total kinetic energy from hydrometeor impacts. (a) Contribution of the top 40 5-minute periods of hail as a fraction of the annual total kinetic energy of hail impacts (b) Contribution of the top 40 5-minute periods of rain as a fraction of the annual total kinetic energy of rain impacts. Cumulative fraction of annual impact kinetic energy from the top X (c) hail events and (d) rain events, where X is set to 40 for hail because no site exhibits more than 36 events per year and is truncated to 100 for rain.

14
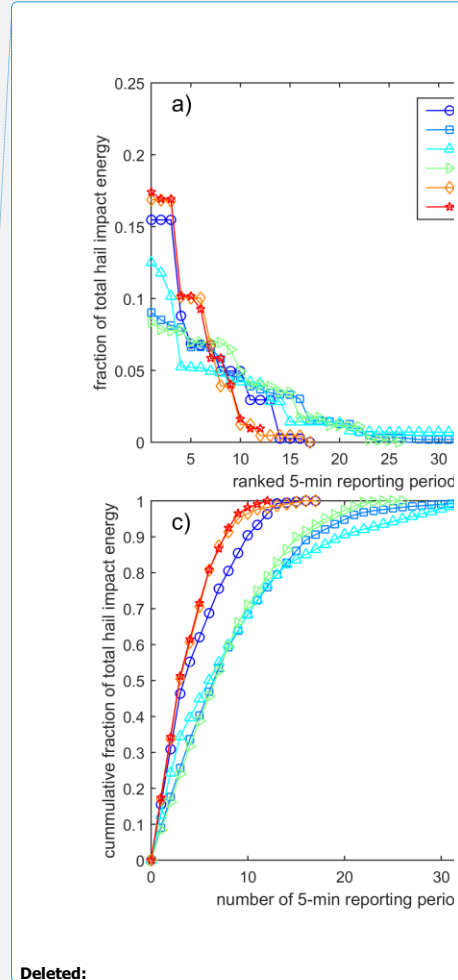
Illustrative examples of uncertainties in impact kinetic energy due to RADAR observational uncertainties in V_{mean}, RR and D_{75} are shown in Fig. 8. For the representative 5-minute period of heavy rain variation of $RR \pm 50\%$, is associated with a $\pm$ 15% variation in kinetic energy of impact (Fig. 8a). Increases or decreases in mean wind speed by 4.2 ms^{-1}, (the upper end of wind speed uncertainty observed in previous work for an elevation angle of 0.5°) (Fast et al., 2008), are shown to decrease
5   kinetic energy, since rotor speed decreases for wind speeds below, or significantly above the rated wind speed of the turbines (Fig. 4c). For a representative period of hail ($D_{75} = 42$ mm and $V_{mean} = 11.3$ ms^{-1}), impact kinetic energy varies by $\pm$ 20% for a $\pm$ 50% variation in V_{mean} and D_{75} (Fig. 8b). Impact kinetic energy actually decreases as D_{75} exceeds 120% of the nominal value ($D_{75} = 42$ mm) (Fig. 8b). This decrease is explained by the interaction of the single parameter exponential hail size distribution (Fig. 4c) and the applied hail diameter ceiling. As D_{75} increases the truncation of the upper tail of the hail distribution (Fig. 8c)
10 means the total modelled mass of hail per unit volume decreases (Fig. 8d).
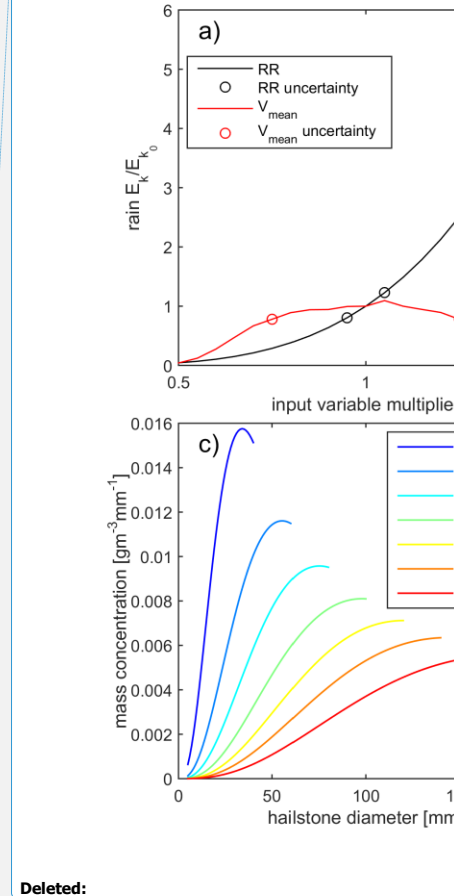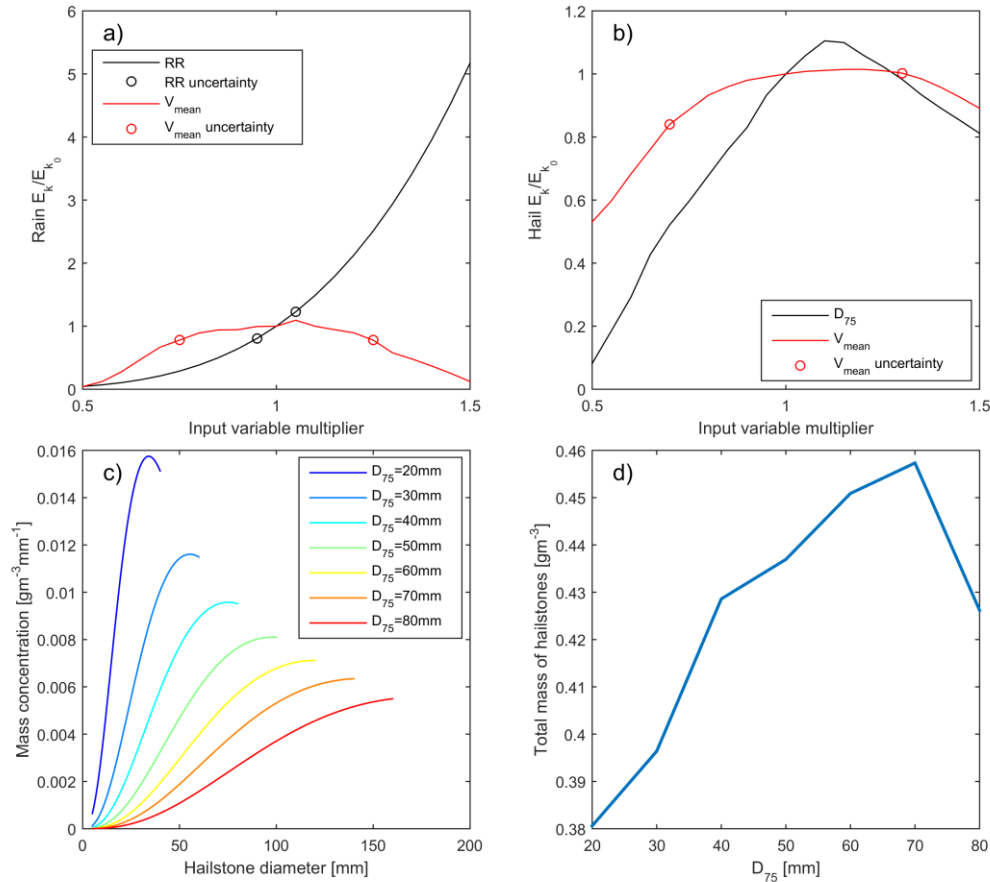
Figure 8 – Sensitivities of rain (a) and hail (b) impact kinetic energies in one 5-minute period to application of ±50% uncertainties on the input parameters; wind speed (V_{mean}) and precipitation intensity (RR) or hail diameter (D_{75}). Circles represent reported uncertainties in RADAR retrievals of wind speed (Fast et al., 2008) and rainfall rate (see Table 1 in (Seo and Krajewski, 2010)). (c) Mass concentrations of hailstones per cubic meter of air (expressed as dM/dD) associated with a range of D_{75} values as a function of hailstone diameter. (d) Total hail mass (in g) per m^3 of air as a function of D_{75}.

4   Conclusions

A robust and flexible framework has been developed and presented for generating an observationally constrained georeferenced assessment of precipitation-induced wind turbine blade leading edge erosion potential. The approach elaborated

herein is naturally subject to a range of uncertainties but is automated, objective, repeatable and predicated on publicly available data available from across most of the continental US. Further, the modular structure means it is flexible to use with different assumptions and/or data streams. Although the data volumes are not trivial (see Appendix A) this analysis framework could be applied to NWS RADAR data to estimate LEE potential at any arbitrary site in CONUS and/or applied to data from other

5 national dual-polarization RADAR networks for other regions of the world. For example, the Network of European Meteorological Services (EUMETNET) operates over 200 RADAR many of which have been upgraded to dual polarization (Saltikoff et al., 2018). The tool proposed here could be used to provide a first assessment of the erosion climate in which a given sited turbine may operate in. It thus provides an important first step towards enabling an assessment of the threat of excessive precipitation-induced LEE in a given deployment environment and the cost-effectiveness of options to reduce the likelihood of

10 premature blade damage.

The actual likelihood of excess WT LEE and blade damage in any environment is not only a function of the precipitation and wind climate, but also the WT dimensions, materials used in the blade coatings and the coating thickness (Eisenberg et al., 2018; Slot et al., 2015), the presence of existing micro-structural defects (Evans et al., 1980) due to manufacturing defects and damage during transportation (Keegan et al., 2013; Nelson et al., 2017) and other aspects of the operating environment

15 (including thermal fatigue and the occurrence of icing (Slot et al., 2015)).

The preliminary estimates of erosion potential and the partitioning between liquid precipitation and hail are naturally subject to limitations including, in likely order of importance:

- The relatively short duration of time for which the dual-polarization RADAR products are available. The upgrade of the NWS RADAR network to dual polarization was completed in April 2013, thus only the complete years of 2014-2018,

20 inclusive were available for analysis. Given the large inter-annual variability in precipitation climates this is too short to build a comprehensive climatology (Karl et al., 1995; Prein and Holland, 2018). Any geospatial depiction of the potential precipitation erosion climate will vary according to the precise data period used to compute the climatology and may evolve as a result of climate non-stationarity altering aspects of the precipitation climate (e.g. probability of hail (Brimelow et al., 2017) and rainfall intensity (Easterling et al., 2000)).

25 - The applicability of the RADAR-derived wind speed estimates to derive wind turbine blade rotational speed. There are considerable challenges to line-of-sight wind retrievals from RADAR (Fast et al., 2008). The approach adopted herein assumes a uniform wind flow pattern to derive the wind speeds at the nominal wind turbine hub-height which may not be realized. As described above, while the wind speed climates at five of the six locations considered exhibited relatively good agreement with previous estimates of wind climates, values for the location in Texas are negatively biased. This likely

30 results in a negative bias in kinetic energy transfer for this site.

- Assumptions regarding the size distribution, occurrence and terminal velocities of hail (Dessens et al., 2015; Allen et al., 2017; Heymsfield et al., 2014). The evolution of the NWS RADAR network to dual polarization provides an unprecedented opportunity for spatial estimates of hail presence and size in clouds (Kumjian et al., 2018). However, hail production is a complex and incompletely understood phenomenon (Dennis and Kumjian, 2017; Blair et al., 2017; Pruppacher and Klett,

35 2010). There are substantial event-to-event variations in the size distribution and density of hail stones (Heymsfield et al., 2014), in the presence of solid-phase hydrometeors in clouds (as detected by RADAR) and the occurrence of hail at the ground (Kumjian et al., 2019). Estimates of hail occurrence, size distribution and terminal fall velocity presented herein are likely conservative (i.e. upper bounds on true values), and thus LEE may be over-estimated.

- Assumptions regarding the size distribution of rain droplets. Most observational studies indicate an exponential form

40 (Uijlenhoet, 2001), and the Marshall-Palmer distribution is the most widely applied. However, a range of different forms

Deleted: of

Deleted: (where RADAR coverage may be less complete than in the US)

Deleted: naturally
Formatted: Indent: First line: 0.3"

Formatted: Indent: First line: 0.25"
Deleted: i

Moved (insertion) [2]
Deleted: and
Field Code Changed
Deleted: occurrence
Field Code Changed
Deleted: and t
Deleted: and
Deleted: and
Deleted: with respect to both properties (i.e. both the frequency and size of hail stones
Deleted: ,
Deleted:)
Moved (insertion) [1]

have been proposed to describe the size spectrum of rain droplets (*dN/dR*) including gamma (Ulbrich, 1983) and lognormal (Feingold and Levin, 1986), an alternative exponential form (Best, 1950) and more complex non-parametric forms (Morrison et al., 2019). There is also evidence that droplet size distributions may exhibit a functional dependence on near-surface wind speed (Testik and Pei, 2017).

5 • Assumptions applied in deriving precipitation intensity and other precipitation properties from RADAR. Notable event-to-event variations in the applicability of Z-R relationships have been reported during rain (Uijlenhoet, 2001; Villarini and Krajewski, 2010).

Future work could address and reduce these uncertainties and adapt this approach to examine different wind turbines (by applying a different RPM curve) and/or to assimilate different atmospheric data and/or incorporate more explicit aspects of

10 materials response. In this analysis we have chosen to focus on an energetic approach in which we compute the accumulated kinetic energy transmitted to the blade leading edge instead of using approaches based on the waterhammer equation that seek to compute the impact pressure and material response to the resulting Rayleigh, shear and compression waves (that are assumed to act independently from each individual impact) (Slot et al., 2015; Dashtkar et al., 2019). It is important to reiterate that the approach adopted here i.e. to compute the maximum total kinetic energy transferred to the blade, which is used here as a proxy

15 for the erosion potential, represents the upper bound on actual kinetic energy transfer since it employs a closing velocity characteristic for the tip of WT rotors, assumes all falling hydrometeors impact the blade, and neglects energy loss during the transfer, 'splash' and bounce of hydrometeors. There are more complex frameworks that can be applied to simulate the pressure and transient stresses on the blade coatings (Mishnaevsky Jr, 2019) and impingement erosion (Amirzadeh et al., 2017a, b). A model of the blade response to precipitation impacts could be incorporated within the analysis framework to examine the

20 probability and time to exceed the (Cumulative) Failure Threshold Energy (Fiore et al., 2015).

This work suggests the dominance of hail as a damage vector for WT blades at all of the sites studied here. This is consistent with indications that deep convection and hail are particularly common in the central US (Cintineo et al., 2012) and of large geographic variability in hail frequency (Ni et al., 2017). This finding emphasizes the key importance of efforts to build and enhance hail climatologies (Allen et al., 2015; Gagne et al., 2019) with applications in a wide range of industries (from insurance

25 to renewable energy). The dominance of hail as a damage vector and the importance of a relatively small number of 5-minute periods to total annual kinetic energy transfer from rain adds credence to the proposal that blade LEE could be greatly reduced by operating erosion-safe turbine control (Bech et al., 2018) wherein the WT are curtailed during periods with extreme precipitation (very heavy rain or the occurrence of hail) without substantial loss of income.

5   Acknowledgments

18

Moved up [1]: <#>Assumptions regarding the size distribution of rain droplets. Most observational studies indicate an exponential form (Uijlenhoet, 2001), and the Marshall-Palmer distribution is the most widely applied. However, a range of different forms have been proposed to describe the size spectrum of rain droplets (*dN/dR*) including gamma (Ulbrich, 1983) and lognormal (Feingold and Levin, 1986), an alternative exponential form (Best, 1950) and more complex non-parametric forms (Morrison et al., 2019). There is also evidence that droplet size distributions may exhibit a functional dependence on near-surface wind speed (Testik and Pei, 2017).¶

Moved up [2]: <#>Assumptions regarding the size distribution and occurrence of hail (Dessens et al., 2015;Allen et al., 2017). The evolution of the NWS RADAR network to dual polarization provides an unprecedented opportunity for spatial estimates of hail occurrence and size in clouds (Kumjian et al., 2018). However, hail production is a complex and incompletely understood phenomenon (Dennis and Kumjian, 2017;Blair et al., 2017;Pruppacher and Klett, 2010) and there are substantial event-to-event variations in the size distribution of hail stones and in the presence of solid-phase hydrometeors in clouds (as detected by RADAR) and the occurrence of hail at the ground (Kumjian et al., 2019). Estimates of hail occurrence and size distribution presented herein are likely conservative with respect to both properties (i.e. both the frequency and size of hail stones may be over-estimated). ¶

Deleted: <#>

Deleted: <#>The applicability of the RADAR-derived wind speed estimates to derive wind turbine blade rotational speed. There are considerable challenges to line-of-sight wind retrievals from RADAR (Fast et al., 2008). The approach adopted herein assumes a uniform wind flow pattern to derive the wind speeds at the nominal wind turbine hub-height which may not be realized. as described herein while the wind speed climates at five of the six locations considered herein exhibited relatively good agreement with previous estimates of wind climates, values for the location in Texas are negatively biased. This likely results in a negative bias in kinetic energy transfer for this site.¶

Deleted: (t

Deleted: may be different for other regions of the world, as convectivitye conditions and hail are especially common in the central US)

Deleted: indicates

Data availability

The USGS Wind Turbine Database used in Figure 1 is available for download from https://eerscmap.usgs.gov/uswtdb/. The NOAA Weather and Climate Toolkit (WCT) is a free, platform independent Java-based software tool distributed from NOAA's National Centers for Environmental Information (NCEI) (download is available from https://www.ncdc.noaa.gov/wct/). The NWS RADAR data are available from download from; https://www.ncdc.noaa.gov/data-access/radar-data.

Appendix A.

The workflow, NWS RADAR data products and data volumes necessary for the components of the precipitation erosion climate are as follows:

1. Download daily .tar archives of NEXRAD polarized Doppler RADAR data using ftp from the data repository hosted at; https://www.ncdc.noaa.gov/nexradinv/. These tar archives contain at 5 minute intervals all NEXRAD level 2 and 3 data and data products, in binary NEXRAD format. The 365 daily tar comprise 60 – 100 GB per station per year (PSPY).
2. Preprocessing
   a. Extract precipitation rates (N1P) and hail reports (NHI) files from each daily tar file.
   b. Import raw files into NOAA Weather and Climate Toolkit (https://www.ncdc.noaa.gov/wct/), translate N1P, N0V and NHI files into netcdf, and .csv, File sizes and numbers
      - Hydrometeor Classification (HHC) raw files (32,000 to 70,000 files PSPY, 124 – 180 MB PSPY)
      - NHI csv files (12,000 to 137,000 files PSPY, totaling 25 – 190 MB PSPY)
      - N1P raw files (68,000 to 90,000 files PSPY, totaling 600 – 900 MB PSPY)
      - N1P netcdf files (130,000 to 150,000 files PSPY, totaling 240 – 290 GB PSPY)
      - Base wind speed (N0V) raw files (40,000 to 60,000 files PSPY, totaling 35-45 GB PSPY)
      - N0V netcdf files (40,000 to 60,000 files PSPY, totaling 900 – 1100 MB PSPY)

Subsequent data analysis is conducted within MATLAB.

Author contributions

SCP and RJB jointly designed the project and obtained the funding and computing resources for the project. FL conducted the majority of the data analysis and developed the figures with input from SCP and RJB. All contributed to writing the paper.

Competing interests

The authors declare they have no conflict of interest.

References

Allen, J. T., and Tippett, M. K.: The characteristics of United States hail reports: 1955-2014, E-Journal of Severe Storms Meteorology, 10, 2015.

Allen, J. T., Tippett, M. K., and Sobel, A. H.: An empirical model relating US monthly hail occurrence to large-scale meteorological environment, Journal of Advances in Modeling Earth Systems, 7, 226-243, 2015.

Allen, J. T., Tippett, M. K., Kaheil, Y., Sobel, A. H., Lepore, C., Nong, S., and Muehlbauer, A.: An extreme value model for US hail size, Monthly Weather Review, 145, 4501-4519, 2017.

Alpert, J. C., and Kumar, V. K.: Radial wind super-obs from the WSR-88D radars in the NCEP operational assimilation system, Monthly weather review, 135, 1090-1109, 2007.

Amirzadeh, B., Louhghalam, A., Raessi, M., and Tootkaboni, M.: A computational framework for the analysis of rain-induced erosion in wind turbine blades, part I: Stochastic rain texture model and drop impact simulations, Journal of Wind Engineering and Industrial Aerodynamics, 163, 33-43, 2017a.

19

Deleted: hourly

Amirzadeh, B., Louhghalam, A., Raessi, M., and Tootkaboni, M.: A computational framework for the analysis of rain-induced erosion in wind turbine blades, part II: Drop impact-induced stresses and blade coating fatigue life, Journal of Wind Engineering and Industrial Aerodynamics, 163, 44-54, 2017b.

Appleby-Thomas, G. J., Hazell, P. J., and Dahini, G.: On the response of two commercially-important CFRP structures to multiple ice impacts, Composite Structures, 93, 2619-2627, 2011.

Auer, A. H.: Distribution of graupel and hail with size, Monthly Weather Review, 100, 325-328, 1972.

AWEA: US wind industry annual market report year ending 2018, American Wind Energy Association, Washington, DC, USA, 2019. https://www.awea.org/resources/publications-and-reports/market-reports/2018-u-s-wind-industry-market-reports.

Bartolomé, L., and Teuwen, J.: Prospective challenges in the experimentation of the rain erosion on the leading edge of wind turbine blades, Wind Energy, 22, 140-151, 2019.

Bech, J. I., Hasager, C. B., and Bak, C.: Extending the life of wind turbine blade leading edges by reducing the tip speed during extreme precipitation events, Wind Energy Science, 3, 729-748, 2018.

Best, A.: The size distribution of raindrops, Quarterly Journal of the Royal Meteorological Society, 76, 16-36, 1950.

Blair, S. F., Laflin, J. M., Cavanaugh, D. E., Sanders, K. J., Currens, S. R., Pullin, J. I., Cooper, D. T., Deroche, D. R., Leighton, J. W., and Fritchie, R. V.: High-resolution hail observations: Implications for NWS warning operations, Weather and Forecasting, 32, 1101-1119, 2017.

Bolinger, M., and Wiser, R.: Understanding wind turbine price trends in the US over the past decade, Energy Policy, 42, 628-641, 2012.

Brimelow, J. C., Burrows, W. R., and Hanesiak, J. M.: The changing hail threat over North America in response to anthropogenic climate change, Nature Climate Change, 7, 516, 2017.

Brøndsted, P., Lilholt, H., and Lystrup, A.: Composite materials for wind power turbine blades, Annu. Rev. Mater. Res., 35, 505-538, 2005.

Brown, M.: Turbine servicing act before the warranty is over. In: Wind Power Monthly, 2010.

Carroll, J., McDonald, A., and McMillan, D.: Failure rate, repair time and unscheduled O&M cost analysis of offshore wind turbines, Wind Energy, 19, 1107-1119, 2016.

Chandrasekar, V., Keränen, R., Lim, S., and Moisseev, D.: Recent advances in classification of observations from dual polarization weather radars, Atmospheric Research, 119, 97-111, 2013.

Changnon, S. A.: Data and approaches for determining hail risk in the contiguous United States, Journal of Applied Meteorology, 38, 1730-1739, 1999.

Changnon, S. A.: Increasing major hail losses in the US, Climatic Change, 96, 161-166, 2009.

Changnon, S. A., Changnon, D., and Hilberg, S. D.: Hailstorms across the nation: An atlas about hail and its damages, Available from: https://www.isws.illinois.edu/pubdoc/CR/ISWSCR2009-12.pdf, 2009.

Cheng, L., and English, M.: A relationship between hailstone concentration and size, Journal of the Atmospheric Sciences, 40, 204-213, 1983.

Cintineo, J. L., Smith, T. M., Lakshmanan, V., Brooks, H. E., and Ortega, K. L.: An objective high-resolution hail climatology of the contiguous United States, Weather and Forecasting, 27, 1235-1248, 2012.

Cortés, E., Sánchez, F., O'Carroll, A., Madramany, B., Hardiman, M., and Young, T. M.: On the Material Characterisation of Wind Turbine Blade Coatings, Materials, 10, 1146, 2017.

Crum, T. D., Saffle, R. E., and Wilson, J. W.: An update on the NEXRAD program and future WSR-88D support to operations, Weather and Forecasting, 13, 253-262, 1998.

Cunha, L. K., Smith, J. A., Krajewski, W. F., Baeck, M. L., and Seo, B.-C.: NEXRAD NWS polarimetric precipitation product evaluation for IFloodS, Journal of Hydrometeorology, 16, 1676-1699, 2015.

Dalili, N., Edrisy, A., and Carriveau, R.: A review of surface engineering issues critical to wind turbine performance, Renewable and Sustainable Energy Reviews, 13, 428-438, http://dx.doi.org/10.1016/j.rser.2007.11.009, 2009.

Dashtkar, A., Hadavinia, H., Sahinkaya, M. N., Williams, N. A., Vahid, S., Ismail, F., and Turner, M.: Rain erosion-resistant coatings for wind turbine blades: A review, Polymers and Polymer Composites, 0967391119848232, 2019.

Dennis, E. J., and Kumjian, M. R.: The impact of vertical wind shear on hail growth in simulated supercells, Journal of the Atmospheric Sciences, 74, 641-663, 2017.

Dessens, J., Berthet, C., and Sanchez, J.: Change in hailstone size distributions with an increase in the melting level height, Atmospheric Research, 158, 245-253, 2015.

Durakovic, A.: COBRA team tackles blade erosion. In: Offshore Wind, 2019.

Easterling, D. R., Meehl, G. A., Parmesan, C., Changnon, S. A., Karl, T. R., and Mearns, L. O.: Climate Extremes: Observations, Modeling, and Impacts, Science, 289, 2068-2074, 2000.

Eisenberg, D., Laustsen, S., and Stege, J.: Wind turbine blade coating leading edge rain erosion model: Development and validation, Wind Energy, 21, 942-951, 2018.

Evans, A., Ito, Y., and Rosenblatt, M.: Impact damage thresholds in brittle materials impacted by water drops, Journal of Applied Physics, 51, 2473-2482, 1980.

Fast, J. D., Newsom, R. K., Allwine, K. J., Xu, Q., Zhang, P., Copeland, J., and Sun, J.: An evaluation of two NEXRAD wind retrieval methodologies and their use in atmospheric dispersion models, Journal of Applied Meteorology and Climatology, 47, 2351-2371, 2008.

20

Feingold, G., and Levin, Z.: The lognormal fit to raindrop spectra from frontal convective clouds in Israel, Journal of climate and applied meteorology, 25, 1346-1363, 1986.

Fiore, G., Camarinha Fujiwara, G. E., and Selig, M. S.: A damage assessment for wind turbine blades from heavy atmospheric particles, 53rd AIAA Aerospace Sciences Meeting, 2015.

5 Froese, M.: Wind-farm owners can now detect leading-edge erosion from data alone, Windpower Engineering and Development, August 14, 2018, 2018.

Gagne, D. J., Haupt, S. E., Nychka, D. W., and Thompson, G.: Interpretable Deep Learning for Spatial Analysis of Severe Hailstorms, Monthly Weather Review, In press, early view available at; https://doi.org/10.1175/MWR-D-1118-0316.1171, 2019.

10 Gaudern, N.: A practical study of the aerodynamic impact of wind turbine blade leading edge erosion, Journal of Physics: Conference Series, 2014, 012031,

Giguère, P., and Selig, M. S.: Aerodynamic effects of leading-edge tape on aerofoils at low Reynolds numbers, Wind Energy, 2, 125-136, 1999.

Herring, R., Dyer, K., Martin, F., and Ward, C.: The increasing importance of leading edge erosion and a review of existing
15   protection solutions, Renewable and Sustainable Energy Reviews, 115, 109382, 2019.

Heymsfield, A. J., Giammanco, I. M., and Wright, R.: Terminal velocities and kinetic energies of natural hailstones, Geophysical Research Letters, 41, 8666-8672, 2014.

Istok, M. J., Fresch, M., Smith, S., Jing, Z., Murnan, R., Ryzhkov, A., Krause, J., Jain, M., Ferree, J., and Schlatter, P.: WSR-88D dual polarization initial operational capabilities, Preprints, 25th Conf. on Interactive Information and Processing Systems
20   for Meteorology, Oceanography, and Hydrology, Phoenix, AZ, Amer. Meteor. Soc, 2009,

Johnson, J., MacKeen, P. L., Witt, A., Mitchell, E. D. W., Stumpf, G. J., Eilts, M. D., and Thomas, K. W.: The storm cell identification and tracking algorithm: An enhanced WSR-88D algorithm, Weather and forecasting, 13, 263-276, 1998.

Karl, T. R., Knight, R. W., and Plummer, N.: Trends in high-frequency climate variability in the twentieth century, Nature, 377, 217, 1995.

25 Keegan, M. H., Nash, D., and Stack, M.: On erosion issues associated with the leading edge of wind turbine blades, Journal of Physics D: Applied Physics, 46, 383001, 2013.

Kelleher, K. E., Droegemeier, K. K., Levit, J. J., Sinclair, C., Jahn, D. E., Hill, S. D., Mueller, L., Qualley, G., Crum, T. D., and Smith, S. D.: Project craft: A real-time delivery system for nexrad level ii data via the internet, Bulletin of the American Meteorological Society, 88, 1045-1058, 2007.

30 Kim, H., and Kedward, K. T.: Modeling hail ice impacts and predicting impact damage initiation in composite structures, AIAA journal, 38, 1278-1288, 2000.

Kumjian, M. R.: Weather radars, in: Remote Sensing of Clouds and Precipitation, edited by: Andronache, C., Springer, 15-63, 2018.

Kumjian, M. R., Richardson, Y. P., Meyer, T., Kosiba, K. A., and Wurman, J.: Resonance Scattering Effects in Wet Hail Observed
35   with a Dual-X-Band-Frequency, Dual-Polarization Doppler on Wheels Radar, Journal of Applied Meteorology and Climatology, 57, 2713-2731, 2018.

Kumjian, M. R., Lebo, Z. J., and Ward, A. M.: Storms Producing Large Accumulations of Small Hail, Journal of Applied Meteorology and Climatology, 58, 341-364, 2019.

Lane, J. E., Sharp, D. W., Kasparis, T. C., and Doesken, N. J.: P2. 10 HAIL DISDROMETER ARRAY FOR LAUNCH SYSTEMS
40   SUPPORT, 12th Conf. on Integrated Observing and Assimilation Systems for the Atmosphere, Oceans and Land Surface; 20-24 Jan. 2008, New Orleans, LA, USA, 2008,

Loomis, I.: Hail causes the most storm damage costs across North America, EOS 99(10)34 2018. doi 10.1029/2018EO104487.

Marshall, J. S., and Palmer, W. M. K.: The distribution of raindrops with size, Journal of meteorology, 5, 165-166, 1948.

Mishnaevsky Jr, L.: Repair of wind turbine blades: Review of methods and related computational mechanics problems, Renewable
45   energy, 140, 828-839, 2019.

Mishnaevsky, L., Branner, K., Petersen, H., Beauson, J., McGugan, M., and Sørensen, B.: Materials for wind turbine blades: an overview, Materials, 10, 1285, 2017.

Moné, C., Hand, M., Bolinger, M., Rand, J., Heimiller, D., and Ho, J.: 2015 Cost of Wind Energy Review, Wind Technologies Office USDoE No. DEAC02-05CH11231., 95 pp., 2017.

50 Morrison, H., Kumjian, M. R., Martinkus, C. P., Prat, O. P., and van Lier-Walqui, M.: A general N-moment normalization method for deriving raindrop size distribution scaling relationships, Journal of Applied Meteorology and Climatology, 58, 247-267, 2019.

Nelson, J. W., Riddle, T. W., and Cairns, D. S.: Effects of defects in composite wind turbine blades–Part 1: Characterization and mechanical testing, Wind Energy Science, 2, 641-652, 2017.

55 Ni, X., Liu, C., Cecil, D. J., and Zhang, Q.: On the detection of hail using satellite passive microwave radiometers and precipitation radar, Journal of Applied Meteorology and Climatology, 56, 2693-2709, 2017.

NOAA: NOAA Next Generation Radar (NEXRAD) Level 2 Base Data., access: January 7, 2019, 1991.

NOAA: Federal Meteorological Handbook, No. 11 WSR-88D Meteorologic Observations Part A, System concepts, responsibilities, and procedures. FCM-H11A-2016. Office of the Federal Coordinator for Meteorological Services,
60   Washington, DC, 2016a.

21

NOAA: Federal Meteorological Handbook, No. 11 WSR-88D Meteorologic Observations Part C, Products and Algorithms. FCM-H11A-2016. Office of the Federal Coordinator for Meteorological Services, Washington, DC, 2016b.

Prat, O., and Nelson, B.: Evaluation of precipitation estimates over CONUS derived from satellite, radar, and rain gauge data sets at daily to annual scales (2002–2012), Hydrology and Earth System Sciences, 19, 2037-2056, 2015.

5 Preece, C. M.: Treatise on Materials Science and Technology, Vol. 16. Erosion, Academic Press, 450 pp., 1979.

Prein, A. F., and Holland, G. J.: Global estimates of damaging hail hazard, Weather and Climate Extremes, 22, 10-23, https://doi.org/10.1016/j.wace.2018.10.004, 2018.

Pruppacher, H. R., and Klett, J. D.: Microphysics of Clouds and Precipitation, Springer, ISBN: 978-0-7923-4211-3, 954 pp., 2010.

Pryor, S. C., Shepherd, T. J., and Barthelmie, R. J.: Interannual variability of wind climates and wind turbine annual energy 10 production, Wind Energy Science, 3, 651-665, 2018.

Pryor, S. C., Shepherd, T. J., Barthelmie, R. J., Hahmann, A. N., and Volker, P. J. H.: Wind farm wakes simulated using WRF, Journal of Physics: Conference Series, 2019.

Rempel, L.: Rotor blade leading edge erosion-real life experiences, Wind Systems Magazine, 11, 22-24, 2012.

Salonen, K., Niemelä, S., and Fortelius, C.: Application of radar wind observations for low-level NWP wind forecast validation, 15 Journal of Applied Meteorology and Climatology, 50, 1362-1371, 2011.

Saltikoff, E., Haase, G., Leijnse, H., Novak, P., and Delobbe, L.: OPERA - past, present and future, 10th European Conference on RADAR in meteorology and hydrology, Ede-Wageningen, The Netherlands, 2018,

Sareen, A., Sapre, C. A., and Selig, M. S.: Effects of leading edge erosion on wind turbine blade performance, Wind Energy, 17, 1531-1542, 2014.

20 Schramm, M., Rahimi, H., Stoevesandt, B., and Tangager, K.: The Influence of Eroded Blades on Wind Turbine Performance Using Numerical Simulations, Energies 10, 1420, 2017.

Seo, B.-C., and Krajewski, W. F.: Scale dependence of radar rainfall uncertainty: Initial evaluation of NEXRAD's new super-resolution data for hydrologic applications, Journal of Hydrometeorology, 11, 1191-1198, 2010.

Seo, B.-C., Dolan, B., Krajewski, W. F., Rutledge, S. A., and Petersen, W.: Comparison of single-and dual-polarization–based 25 rainfall estimates using NEXRAD data for the NASA Iowa Flood Studies project, Journal of Hydrometeorology, 16, 1658-1675, 2015.

Shohag, M. A. S., Hammel, E. C., Olawale, D. O., and Okoli, O. I.: Damage mitigation techniques in wind turbine blades: A review, Wind Engineering, 41, 185-210, 2017.

Shokrieh, M. M., and Bayat, A.: Effects of ultraviolet radiation on mechanical properties of glass/polyester composites, Journal of 30 Composite materials, 41, 2443-2455, 2007.

Slot, H., Gelinck, E., Rentrop, C., and van der Heide, E.: Leading edge erosion of coated wind turbine blades: Review of coating life models, Renewable Energy, 80, 837-848, 2015.

Straka, J. M., Zrnić, D. S., and Ryzhkov, A. V.: Bulk hydrometeor classification and quantification using polarimetric radar data: Synthesis of relations, Journal of Applied Meteorology, 39, 1341-1372, 2000.

35 Stull, R.: Meteorology for scientists and engineers, Brooks/Cole, Univ. of British Columbia, 938 pp., 2015. isbn 978-0-88865-178-5

Testik, F. Y., and Pei, B.: Wind effects on the shape of raindrop size distribution, Journal of Hydrometeorology, 18, 1285-1303, 2017.

Traphan, D., Herráez, I., Meinlschmidt, P., Schlüter, F., Peinke, J., and Gülker, G.: Remote surface damage detection on rotor 40 blades of operating wind turbines by means of infrared thermography, Wind Energy Science, 3, 639-650, 2018.

U.S. Energy Information Administration: Electric Power Annual 2017, U.S. DoE, Washington D.C.: https://www.eia.gov/electricity/annual/pdf/epa.pdf, 239 pp pp., 2018.

Uijlenhoet, R.: Raindrop size distributions and radar reflectivity–rain rate relationships for radar hydrology, Hydrology and Earth System Sciences, 5, 615-628, 2001.

45 Ulbrich, C. W.: Natural variations in the analytical form of the raindrop size distribution, Journal of climate and applied meteorology, 22, 1764-1775, 1983.

Valaker, E. A., Armada, S., and Wilson, S.: Droplet erosion protection coatings for offshore wind turbine blades, Energy Procedia, 80, 263-275, 2015.

Villarini, G., and Krajewski, W. F.: Review of the different sources of uncertainty in single polarization radar-based estimates of 50 rainfall, Surveys in Geophysics, 31, 107-129, 2010.

Wilson, J. W., and Brandes, E. A.: Radar measurement of rainfall—A summary, Bulletin of the American Meteorological Society, 60, 1048-1060, 1979.

Wiser, R., Jenni, K., Seel, J., Baker, E., Hand, M., Lantz, E., and Smith, A.: Expert elicitation survey on future wind energy costs, Nature Energy, 1, 16135, 10.1038/nenergy.2016.135, 2016.

55 Wiser, R., and Bolinger, M.: 2017 Wind Technologies Market Report, DOE/EE-1798, Office of Energy Efficiency & Renewable Energy, U.S. Department of Energy. Available online from: https://www.energy.gov/sites/prod/files/2018/08/f54/2017_wind_technologies_market_report_8.15.18.v2.pdf, 81, 2018.

Witt, A., Eilts, M. D., Stumpf, G. J., Johnson, J., Mitchell, E. D. W., and Thomas, K. W.: An enhanced hail detection algorithm for the WSR-88D, Weather and Forecasting, 13, 286-303, 1998.

22

Zhang, S., Dam-Johansen, K., Nørkjær, S., Bernad Jr, P. L., and Kiil, S.: Erosion of wind turbine blade coatings–design and analysis of jet-based laboratory equipment for performance evaluation, Progress in Organic Coatings, 78, 103-115, 2015.

Zhu, F., and Li, F.: Reliability analysis of wind turbines, in: Stability Control & Reliable Performance of Wind Turbines, DOI: 10.5772/intechopen.74859 2018.

5

Formatted: Indent: Left: 0"